Numerical Investigation of Reflection Process of FRC

Takashi Kanki
Japan Coast Guard Academy,
5-1 Wakaba, Kure, Hiroshima 737-8512, Japan

Abstract

A two-dimensional magnetohydrodynamic (MHD) simulation of a reflection dynamics on a field-reversed configuration (FRC) plasma is performed by numerically modeling a confinement region of the FRC Injection Experiment (FIX) machine. The FRC plasma is reflected by a downstream magnetic mirror field at the end of the confinement region without severe destruction of the closed magnetic flux surfaces even when injected with supersonic velocity into the magnetic mirror region, showing the robustness of the FRC against external perturbations. By examining details of the FRC motion, it is also predicted for any translation velocities that the FRC eventually settles down in the confinement region and approaches MHD equilibrium condition. Interestingly, it is observed that formation of a discontinuous wave front is caused by a shock when the FRC with supersonic velocity is reflected by the magnetic mirror.

I. INTRODUCTION

A field-reversed configuration (FRC) plasma [1] can be translated axially since it is not linked by material objects. Axial translation has offered an attractive and essential ingredient in present experiments as well as an engineering convenience in D-^{3}He fuelled FRC fusion reactor studies in which the start-up, heating, and burn chamber section can be physically separated. For this motivation, many experiments of translation have been carried out.

In the translation experiment on the FRC Injection Experiment (FIX) machine [2] at Osaka, FRC plasma is created in a source region by a field-reversed theta-pinch method, and is injected into an adjacent confinement region with magnetic mirror fields at either end. The injected FRC moves along the magnetic field of the confinement region at supersonic velocity. Subsequently, the FRC reflects at the downstream magnetic mirror. The reflected FRC moves back toward the source region and reflects at the upstream magnetic mirror. It eventually settles down the center of the confinement region without severe degradation of the confinement. As the result, the FRC translation has been successfully achieved by empirically adjusting the confining magnetic field. However, it is observed in the first reflection from the downstream mirror that the separatrix radius of the FRC expands excessively when the confining field is reduced, and that more energy of the translated FRC is lost in the case where the translation velocity is larger and the magnetic mirror ratio is smaller. Details concerning how such a reflection process of a FRC plasma is performed by interaction with the magnetic mirror field remain unclear.

Under this experimental background, the purpose of this study is to investigate the fundamental physics of reflection dynamics of a FRC plasma by means of an axisymmetric numerical simulation. In particular, we will focus our attention to examine the time evolution of the poloidal flux contours and the velocity fields. In addition, we explore the effects of the magnetic mirror field on FRC plasmas.

II. NUMERICAL MODEL OF CONFINEMENT REGION

As shown in Fig. 1, the confinement region in the FIX machine consists of the central confinement region and the mirror field region at its two ends. The central confinement region is 0.8 m inner diameter and 3 m long metal chamber. The confining magnetic field of this region is generated by solenoid coils. The strength of this magnetic field in vacuum B_0 ranges from 0.01 to 0.08 T. In our simulation, we fix B_0 at 0.04 T for typical experimental parameter. The both ends of confinement region are tapered to the 0.5 m inner diameter. In the FIX experiment, the typical strength of the upstream and downstream magnetic mirror fields B_m are 0.13 and 0.17 T, respectively. In the simulation, however, we set $B_m = 0.1$ T as the strength of upstream mirror field, and change that of downstream mirror field. Hence, the mirror ratio R_m at the downstream region varies in accordance with the strength of downstream mirror field. Here, R_m is defined as the ratio of the maximum vacuum mirror field to the confining field in the central part of the confinement region.

Let us use a cylindrical coordinate (z, r, ϕ) in which the z-axis lies along the symmetry axis of the confinement chamber. We assume the axisymmetry, and carry out numerical simulations in a two dimensional (z, r) plane. As shown in Fig. 1, we divide the confinement region in which the simulation is performed into two regions. One is a vacuum subregion where the magnetic field is calculated only, and the other is a plasma subregion where the full set of magnetohydrodynamic (MHD) equations are solved. We use a perfect conducting boundary at the chamber wall. Further, free boundary conditions are imposed on the open ends of confinement region, in order to reduce the reflection of MHD flow. Since in general, a FRC has the sharp plasma pressure gradients in the vicinity of separatrix, we employ a Lagrangian mesh, so as to allow a concentration of the mesh in that region [3]. Furthermore, a two temperature MHD model [4], which calculates electron and ion separately, is used, since the electron-ion energy transfer time in the confinement region is much longer than the time scale of the reflection. The Lagrangian MHD equations are as follows:

$$\frac{d\rho}{dt} = -\rho\nabla\cdot\mathbf{v}, \tag{1}$$

$$\frac{d\mathbf{v}}{dt} = \frac{1}{\rho}\left[-\nabla p + \mathbf{j}\times\mathbf{B}\right], \tag{2}$$

$$\frac{d\mathbf{B}}{dt} = (\mathbf{B}\cdot\nabla)\,\mathbf{v} - \mathbf{B}\,(\nabla\cdot\mathbf{v}) - \nabla\times(\eta\mathbf{j}), \tag{3}$$

$$\frac{d\epsilon_i}{dt} = \frac{1}{\rho_i}\left[-p_i\,(\nabla\cdot\mathbf{v}) - \nabla\cdot\mathbf{q}_i + Q_i\right], \tag{4}$$

$$\frac{d\epsilon_e}{dt} = \frac{1}{\rho_e}\left[-p_e\,(\nabla\cdot\mathbf{v}) - \nabla\cdot\mathbf{q}_e + Q_e\right], \tag{5}$$

where $\rho(=\rho_e+\rho_i)$ is total mass density, $\mathbf{v}$ is fluid velocity, $\mathbf{B}$ is magnetic field, $\mathbf{j}(=\nabla\times\mathbf{B}/\mu_0)$ is electrical current density, $\epsilon(=\epsilon_e+\epsilon_i)$ is total specific internal energy, $p(=p_e+p_i)$ is total pressure, $\mathbf{q}(=\mathbf{q}_e+\mathbf{q}_i)$ is total heat flow, and η is the electrical resistivity due to classical electron collisions. In addition, ρ_α, p_α, ϵ_α, and $\mathbf{q}_\alpha$ refer to the appropriate electron or ion quantities, and Q_i and Q_e represent the Braginskii electron-ion energy equilibration and Joule heating terms [5]. The effects of unequal parallel and perpendicular thermal conduction, which follow Braginskii, are included for both the electrons and the ions [5]. Resistive diffusion of the magnetic field is calculated using classical resistivity. Details of the numerical method have been described elsewhere [6, 7].

Finally, as the initial value for the simulation, we use a numerically computed MHD equilibrium with separatrix radius (normalized by the wall radius at $z = 0$), $x_s \simeq 0.4$ such, as is typically observed in the FIX experiment [8]. The MHD equilibrium of a FRC is described by the Grad-Shafranov equation for the poloidal flux function ψ,

$$r\frac{\partial}{\partial r}\left(\frac{1}{r}\frac{\partial \psi}{\partial r}\right) + \frac{\partial^2 \psi}{\partial z^2} = -r^2\frac{dp}{d\psi}, \tag{6}$$

where p denotes the plasma pressure. In order to solve Eq. (6) numerically under the boundary conditions in the region indicated in Fig. 1, a profile of $dp/d\psi$ must be assumed. As the profile, we take

$$\frac{dp}{d\psi} = \begin{cases} -c(1+\xi\psi) & \text{for} \quad \psi < 0, \\ -cd & \text{for} \quad 0 \leq \psi < \psi_0, \\ 0 & \text{for} \quad \psi_0 \leq \psi. \end{cases} \tag{7}$$

Here c, ξ and d are constants, and ψ_0 is the value of ψ on the vacuum-plasma interface. Note that in Eq. (7) we have $\psi < 0$ inside the separatrix and $\psi \geq 0$ outside the separatrix. FRC equilibria are given by solving the finite difference equation for Eq. (7) using the SOR method; details are found in ref. 8. By applying the thermodynamic equation of an ideal fluid, the plasma density profile can be estimated, assuming that the temperature is spatially uniform in the plasma region. Also, we provide the initial axial velocity, v_z that is spatially constant in the plasma region because of assuming that the FRC plasma is in equilibrium, even when it is translating. The parameters of the initial condition for the simulation are listed in Table 1.

III. NUMERICAL RESULTS

We present the numerical results for the reflection dynamics of a FRC plasma at the downstream mirror region. Time evolution of the poloidal flux contours and the velocity fields is shown in Fig. 2 for the mirror ratio, $R_m = 2.56$ at the downstream region, and the initial axial velocity, $v_z = 5.0 \times 10^4$ m/s. Here, the plasma region is plotted only in the poloidal plane. Also, this initial axial velocity is smaller than the sound velocity of 9.0×10^4 m/s on the separatrix. Hence, this case is the translation with subsonic speed. The top panel in Fig. 2 represents the initial poloidal flux contours and velocity fields before the reflection process, which are an equilibrium with the initial axial velocity of the FRC. The FRC moves towards the downstream region along the confining field and the front part of this arrives there at about $t = 20$ μs. Then as the result of interaction with the magnetic mirror, the separatrix radius begins to expand in this front part, while the rear part of the FRC continues to travel toward the downstream region. Therefore, the FRC is compressed axially by 46% until about $t = 50$ μs. Due to this axial compression, the separatrix radius expands in the downstream region. However, during this compression, the x-point in the downsteam region does not move. After this compression is completely done, the FRC begins to expand axially toward the upstream region. Finally, the FRC gradually leaves the downstream mirror and then is reflected. It is also observed that the pressure wave is propagating along the magnetic field lines outside the separatrix. The phase velocity of this compressional wave is 9.0×10^4 m/s, which is the same as the sound velocity. It is suggested that this wave is the sound wave.

Next, we show the poloidal flux contours and the velocity fields in Fig. 3 for the mirror ratio, $R_m = 3.0$ at the downstream region, and the initial axial velocity, $v_z =$

1.5×10^5 m/s. This case is the translation with supersonic speed. This translation velocity, $v_z \leq 2.0 \times 10^5$ m/s is observed in the FIX experiment for $B_0 = 0.04$ T. The FRC plasma travels towards the downstream region and the front part of this arrives there at about $t = 10$ μs. Then as the result of strong interaction with the magnetic mirror, this front part is compressed, not only axially but also radially until about $t = 20$ μs. Also, the whole FRC shrinks axially by 80%. This axial contraction lasts until about $t = 25$ μs, and then the separatrix radius expands in the vicinity of the central part of the FRC. At this time, excessive expansion of the separatrix radius does not occur regardless of significant volume compression since the FRC deeply creeps into the mirror region. Subsequently, a front part of the FRC has passed through the downstream region. After $t = 20$ μs, a precursor plasma inside the separatrix ($z > 2.2$ m) passes through the downstream region, while the following plasma ($z < 2.2$ m) reflects from the mirror and then goes back towards the upstream region. The opposite direction of plasma flow can stretch out the magnetic field lines, and these field lines at axial position $(z, r) = (2.2$ m, 0.04 m$)$ reconnect at about $t = 30$ μs. Due to this magnetic reconnection, axial plasma flow is found in the end of the downstream region. This suggests that the magnetic mirror may play a role in triggering the magnetic reconnection in the case where the translation velocity is larger. Actually, in the experiment, considerable diamagnetic signals measured by magnetic probes have been observed behind mirror field when the FRC is reflected. After about $t = 35$ μs, the FRC expands again towards the upstream region and leaves the downstream mirror. In this reflection process, the FRC collides with the magnetic mirror at supersonic velocity. The severe destruction of the FRC is not observed regardless of this fact, and the FRC still maintains most of its closed magnetic field configuration. Therefore, this suggests that the FRC plasma is robust against external perturbations. It is also observed at about $t = 40$ μs that a shock wave at speed, 1.4×10^5 m/s is propagating across the magnetic field lines inside the separatrix.

Figure 4 shows the time evolution of the average axial velocity, $< v_z >$ on the midplane ($z = 0.0$ m). The value of $< v_z >$ is obtained by taking an average of axial flows on the midplane. As the translation velocity is increased, $< v_z >$ decreases rapidly at about $t = 40$ μs. The dip of $< v_z >$ at about $t = 40$ μs is attributed to the reflected plasma flows coming back to the midplane. This discontinuity of $< v_z >$ is generated in the case that the translation velocity exceeds the sound velocity. Therefore, this suggests that the formation of the discontinuous front is caused by a shock wave when the plasma is reflected by the magnetic mirror. This discontinuous wave front corresponds to the shock wave as shown in Fig. 3. This observation implies that the fast magnetosonic wave induced within the FRC may steepen to form shock.

Figure 5 shows the time evolution of the average velocity, $< v >$ inside the separatrix. It is shown for any translation velocities that the reflected FRC moves slower than the injected FRC. All reflections are inelastic, and the rebound coefficient e in the translation case of supersonic and subsonic velocities are calculated to be 0.56 and 0.61, respectively. This prediction form the MHD simulation is in agreement with the magnitude of the translation velocity observed in the FIX experiment which is reduced by 40% to 70% after the first reflection [2]. Also, onset of the reflection is evaluated by a zero point of the average velocity. In the translation case of supersonic velocity, $v_z = 1.5 \times 10^5$ m/s, the increase of the average velocity, $< v >$ after about $t = 60$ μs is due to the effect of the second reflection at the upstream magnetic mirror.

In order to examine the dependence of the motion of the FRC during reflection on the translation velocity, we plot the temporal evolution of the spatially averaged force

$< |\mathbf{j} \times \mathbf{B} - \nabla p| >$ in Fig. 6. It is illustrated for any translation velocities that the configuration is far out of MHD equilibrium condition of $\mathbf{j} \times \mathbf{B} = \nabla p$ in the reflection process. Until about $t = 20$ μs, there is a strong deceleration of the FRC due to the magnetic mirror. Thereafter the average force essentially approaches zero. In the translation case of supersonic velocity, $v_z = 1.5 \times 10^5$ m/s, the average force has peaked value at about $t = 70$ μs due to the effect of the second reflection at the upstream magnetic mirror. It is predicted for any translation velocities that the FRC eventually settles down in the confinement region and approaches MHD equilibrium condition.

Figures 7 and 8 show the radial profiles of the plasma pressure and the toroidal current density on the midplane. It is found from Fig. 7 that after the reflection through the supersonic velocity, the pressure profile becomes broader in the peaked part and that the pressure gradients near the separatrix become sharper. It is seen from Fig. 8 that the toroidal current density profile becomes more hollow after the reflection through the supersonic velocity. The discontinuity of the current density profile outside the separatrix before reflection is due to the assumption of function form of pressure profile in the Grad-Shafranov equation.

IV. CONCLUSIONS

We have investigated the dynamics of a reflection process on a FRC plasma by using an axisymmetric MHD simulation. As an initial state we use a MHD equilibrium configuration such as is typically observed in FIX experiment. We give an appropriate initial velocity for the equilibrium configuration. It is found from the simulation results that remarkably, in this reflection process, the FRC still maintains most of its closed magnetic field configuration even when injected with supersonic velocity into the magnetic mirror region, showing the robustness of the FRC against external perturbations. This is a significant feature of the FRC.

From the temporal evolution of the spatially averaged force $\mathbf{j} \times \mathbf{B} = \nabla p$, it is predicted for any translation velocities that the FRC eventually settles down in the confinement region and approaches MHD equilibrium condition. Also, it is found from the time evolution of the average axial velocity, $< v_z >$ on the midplane that the formation of the discontinuous front can be caused by a shock wave when the FRC with supersonic velocity is reflected by the magnetic mirror.

References

[1] M. Tuszewski, Nucl. Fusion **28**, 2033 (1988).

[2] H. Himura *et al.*, Phys. Plasmas **2**, 191 (1995).

[3] J. U. Brackbill and W. E. Pracht, J. Comp. Phys. **13**, 455 (1973).

[4] R. D. Milroy and J. U. Brackbill, Phys. Fluids **25**, 775 (1982).

[5] S. I. Braginskii, *Reviews of Plasma Physics* (edited by M. A. Leontovich, Consultants Bureau, New York, 1965) Vol. **1**, p. 205.

[6] T. Kanki *et al.*, Phys. Plasmas **6**, 4612 (1999).

[7] T. Kanki, IEEE Trans. Magn. **38**, 1205 (2002).

[8] Y. Suzuki *et al.*, Phys. Plasmas **7**, 4062 (2000).

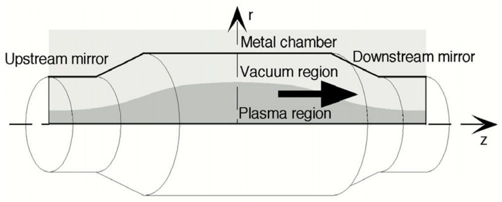

FIG. 1. Schematic diagram of the computation region in cylindrical coordinates (z, r, ϕ), corresponding to the confinement region in the FIX machine. The shaded poloidal plane shows the two dimensional simulation region.

TABLE 1. Parameters for Initial Plasma Condition

Parameter	**Initial Value**
Separatrix Radius r_s	0.17 m
Separatrix Length l_s	3.15 m
Average Mass Density ρ	2.2×10^{-7} kg/m^3
Axial Velocity v_z	1.5×10^{5} m/s
Radial Velocity v_r	0.0 m/s
Ion Temperature T_i	50.0 eV
Electron Temperature T_e	50.0 eV
Confining Magnetic Field B_0	0.04 T

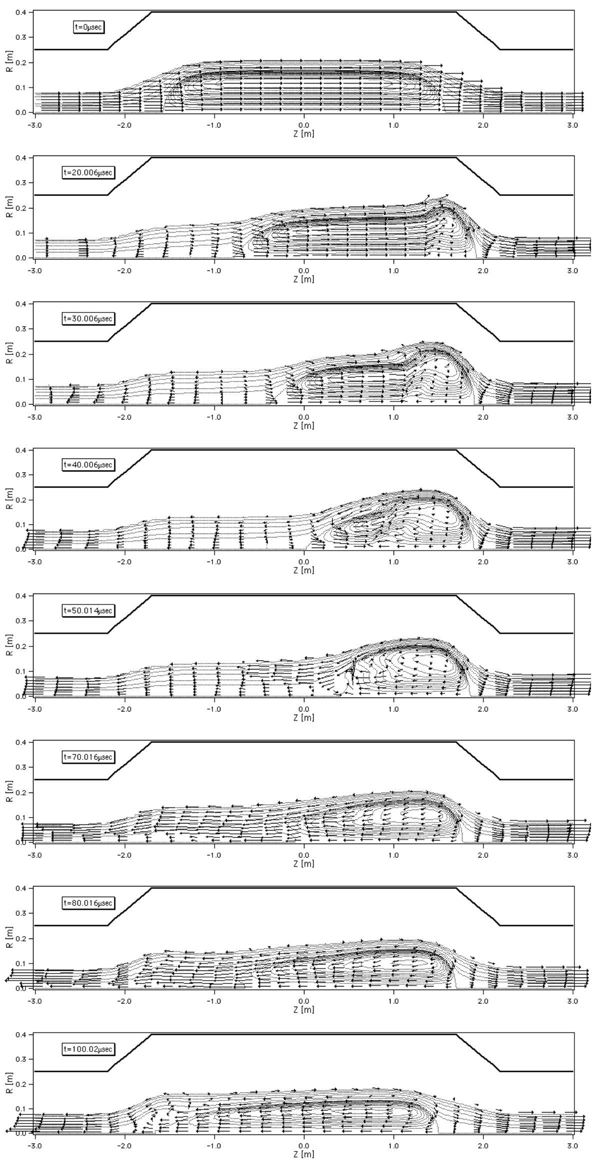

FIG. 2. Time evolution of the poloidal flux contours and the velocity fields of the FRC for the parameter with $R_m = 2.56$ and $v_z = 5.0\times 10^4$ m/s. The dotted lines and the arrows represent flux contours and flow vectors, respectively.

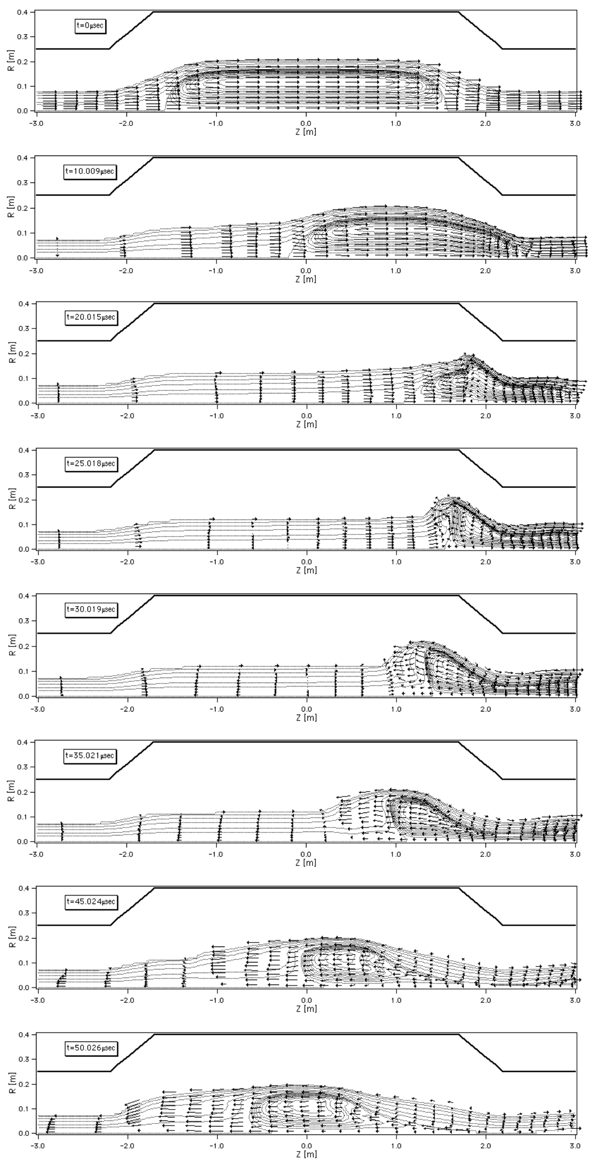

FIG. 3. Time evolution of the poloidal flux contours and the velocity fields of the FRC for the parameter with $R_m = 3.0$ and $v_z = 1.5\times 10^5$ m/s. The dotted lines and the arrows represent flux contours and flow vectors, respectively.

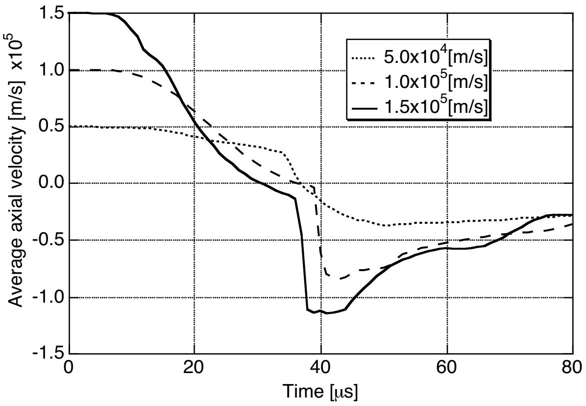

FIG. 4. Time evolution of the average axial velocity $< v_z >$ on the midplane (z = 0.0 m) for the translation velocities: 5.0×10^4, 1.0×10^5 and 1.5×10^5 m/s.

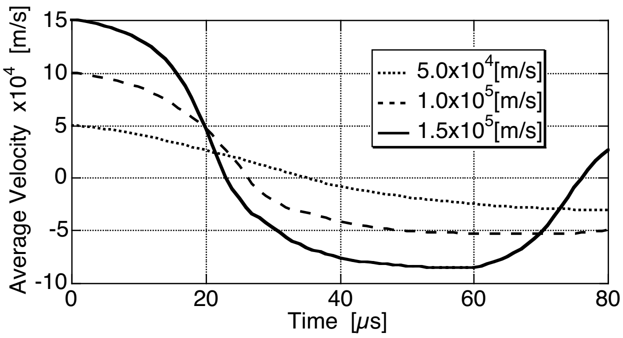

FIG. 5. Time evolution of the average velocity $< v >$ inside the separatrix for the same parameters as Fig. 4.

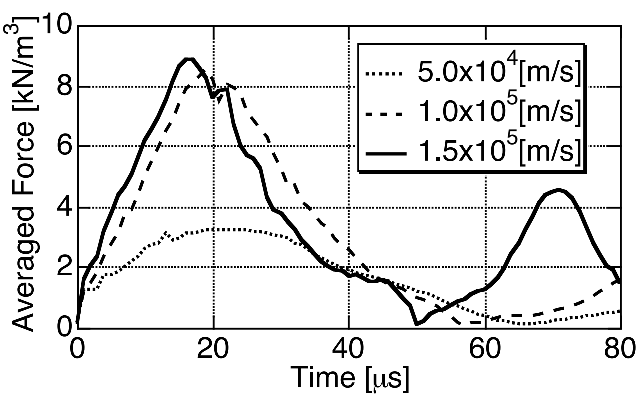

FIG. 6. Time evolution of the spatially averaged force $<|\, \mathbf{j}\times\mathbf{B} - \nabla p \,|>$ for the same parameters as Fig. 4. Here **j**, **B** *and p denote the current density, magnetic field and plasma pressure, respectively.*

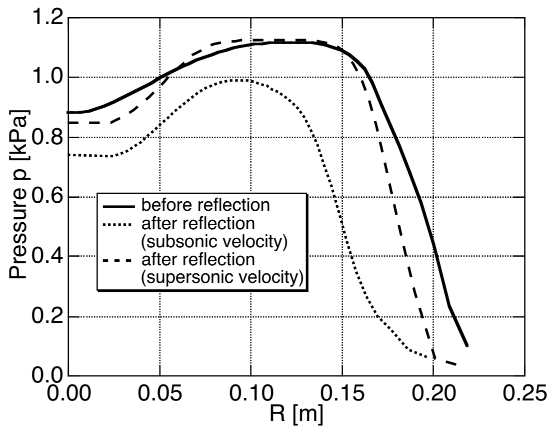

FIG. 7. Radial profile of the plasma pressure p before and after reflection on the midplane.

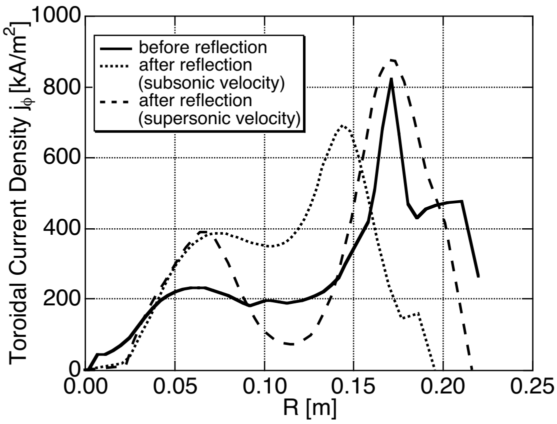

FIG. 8. Radial profile of the toroidal current density j_ϕ before and after reflection on the midplane.